Journal of Alzheimer's Disease 72 (2019) 161–180
DOI 10.3233/JAD-190572
IOS Press

Long-Term Effects of Traumatic Brain Injury in a Mouse Model of Alzheimer's Disease

Marlena Zyśk[a], Fredrik Clausen[b], Ximena Aguilar[a], Dag Sehlin[a], Stina Syvänen[a] and Anna Erlandsson[a,*]
[a]*Department of Public Health and Caring Sciences, Uppsala University, Rudbeck Laboratory, Uppsala, Sweden*
[b]*Department of Neuroscience, Uppsala University, Rudbeck Laboratory, Uppsala, Sweden*

Accepted 21 August 2019

Abstract. Alzheimer's disease (AD) is the leading cause of dementia worldwide, affecting over 10% of the elderly population. Epidemiological evidence indicates that traumatic brain injury (TBI) is an important risk factor for developing AD later in life. However, which injury-induced processes that contribute to the disease onset remains unclear. The aim with the present study was to identify cellular processes that could link TBI to AD development, by investigating the chronic impact of two different injury models, controlled cortical impact (CCI) and midline fluid percussion injury (mFPI). The trauma was induced in 3-month-old tg-ArcSwe mice, carrying the Arctic mutation along with the Swedish mutation, and the influence of TBI on AD progression was analyzed at 12- and 24-weeks post-injury. The long-term effect of the TBI on memory deficiency, amyloid-β (Aβ) pathology, neurodegeneration and inflammation was investigated by Morris water maze, PET imaging, immunohistochemistry, and biochemical analyses. Morris water maze analysis demonstrated that mice subjected to CCI or mFPI performed significantly worse than uninjured tg-ArcSwe mice, especially at the later time point. Moreover, the injured mice showed a late upregulation of reactive gliosis, which concurred with a more pronounced Aβ pathology, compared to uninjured AD mice. Our results suggest that the delayed glial activation following TBI may be an important link between the two diseases. However, further studies in both experimental models and human TBI patients will be required to fully elucidate the reasons why TBI increases the risk of neurodegeneration.

Keywords: Alzheimer's disease, amyloid-β, inflammation, Morris water maze, neurodegeneration astrocytes, PET, traumatic brain injury

INTRODUCTION

Alzheimer's disease (AD) is the most common form of dementia, estimated to affect around 50 million people worldwide [1]. Due to the fact that AD is a progressive neurodegenerative disorder, developing over several years, the pathophysiology of the disease is very complex. The key neuropathological hallmarks of AD are the extracellular plaques, mainly consisting of aggregated amyloid-β (Aβ), and the intracellular neurofibrillary tangles, composed of hyperphosphorylated tau (*p*-tau). In addition, oxidative stress, apoptosis, and neuroinflammation are elevated during the course of the disease [2].

It has been demonstrated that there is a clear epidemiological association between traumatic brain injury (TBI) and AD [3], but the mechanism behind this link is still unclear. Interestingly, Aβ plaques may be found in patients within hours following TBI [4]. If these injury-induced plaques are temporary or result in permanent Aβ pathology is not clear.

*Correspondence to: Anna Erlandsson, Department of Public Health and Caring Sciences/Molecular Geriatrics, Rudbeck Laboratory, Uppsala University, SE-751 85 Uppsala, Sweden. E-mail: anna.erlandsson@pubcare.uu.se.

ISSN 1387-2877/19/$35.00

Since the onset of AD often occurs many years after TBI, long-term cellular mechanisms, such as chronic inflammation, most likely play a central role in the process. In addition to TBI, some of the known risk factors for AD include hypertension and diabetes, which display vascular morbidities [5], indicating that the vascular system of the brain is important for the development of the disease. Several studies suggest that brain tissue damage following TBI is a chronic process with ongoing brain tissue atrophy for several years after the primary injury [6, 7]. Despite that, most TBI studies concentrate on the first weeks following injury and very little is known about the inflammation at later time points. However, it has been reported that both reactive astrocytes and macrophages/microglia are still present in the injured brain one year following trauma in rats [8].

A number of TBI studies have reported effects on cognition and changes in Aβ or tau pathology in mouse models of AD [9–19]. Especially, the short-term effect of TBI has been in focus and only a few investigations have included later time points [9, 10]. None of these studies followed the animals longer than 16 weeks after the inflicted brain trauma or addressed the effect on glial activation at later time points.

Here, we aimed to study the impact of two different TBI models in tg-ArcSwe mice up to 24 weeks following the injury. In order to examine both focal and diffuse aspects of TBI, we use one mostly focal model, controlled cortical impact (CCI), and one mostly diffuse model, midline fluid percussion injury (mFPI). As this is the first long-term study on TBI in tg-ArcSwe mice, we designed the experiments in this way, to not miss an effect elicited by either type of TBI. The tg-ArcSwe mice show elevated levels of soluble Aβ aggregates already at a very young age and develop plaque pathology from around 6-7 months of age [20, 21]. The trauma was induced when the animals were 3 months old, which is prior to any visible Aβ pathology. The first investigated time point, when animals were 6 months old (12 weeks following TBI), coincides with the first appearance of plaques in uninjured tg-ArcSwe mice and the second time point, when the animals were 9 months old (24 weeks following TBI), coincides with pronounced Aβ pathology in uninjured tg-ArcSwe mice.

The two trauma models cause different damage to the brain; while CCI results in a local ipsilateral cortical contusion with scattered neuronal loss in the underlying hippocampus, mFPI results in widespread axonal injury throughout the brain [22]. Using immunohistochemistry, biochemical analyses, Morris water maze (MWM), and PET imaging, we could demonstrate that the Aβ burden and astrocyte gliosis were clearly increased in injured tg-ArcSwe mice compared to uninjured tg-ArcSwe control mice, 24-weeks post-TBI. Notably, there was no elevated pathology at 12 weeks after the injury. These results were in line with our findings that the injured animals showed increased neurodegeneration and severe memory deficiency at the latest time point.

MATERIALS AND METHODS

Animals

Transgenic mice carrying the Arctic (E693G) and Swedish (KM670/6701NL) amyloid-β precursor protein (AβPP) (tg-ArcSwe mice) were obtained by in-house breeding on a C57bl/6J background. The tg-ArcSwe mice develop Aβ deposits in the brain that resemble AD neuropathology. More specifically, the tg-ArcSwe mice express elevated levels of soluble Aβ aggregates, such as Aβ protofibrils, accumulate Aβ inside neurons, and develop robust amyloid plaques. In total 51 gender balanced tg-ArcSwe mice were included in the study, 27 males and 24 females. However, 11 mice died before the experiment was finalized (during the 6 months). Hence, the total number of animals that were included in the MWM study and the immunohistochemistry analysis were 40 animals. The following groups were included: 14 naïve mice (7 of these were sacrificed at 3 months and 7 were sacrificed at 6 months), 12 CCI mice (7 of these were sacrificed at 3 months and 5 were sacrificed at 6 months), and 14 mFPI mice (6 of these were sacrificed at 3 months and 8 were sacrificed at 6 months). The mice analyzed with PET were the same individuals that were included in the MWM test and then euthanized at 6 months. Hence, PET scans were obtained for 7 naïve, 5 CCI, and 8 mFPI, but two PET scans of naïve mice were omitted due to technical problems. The animals that were euthanized at 3 months did not undergo PET scanning. The mice were housed at the National Veterinary Institute in Uppsala at 20–22°C, with access to food and water *ad libitum* on a 12 h light/dark cycle. All experiments were approved by the Uppsala County Animal Ethics board, and followed the rules and regulations of the Swedish Animal Welfare Agency (approval number C17/13). An experimental outline is shown in Supplementary Figure 1A.

Anesthesia

Anesthesia was induced with inhalation of 4% isoflurane in air. During surgery, general anesthesia was maintained with a mix of isoflurane (1.2–1.4%) and N_2O/O_2 (70/30%), delivered through a nose cone. Lubricant eye ointment (Viscotears; Novartis, Basel, Switzerland) was used for corneal protection during the procedure. After being shaved and cleaned with ethanol on the scalp, the mice were placed in a stereotaxic frame and core temperature was maintained at 37°C, using a heating pad controlled by a rectal thermometer. Local anesthesia (Marcain, AstraZeneca, Sweden) was applied to the scalp and the skull was exposed by an incision along the midline. Uninjured controls did not undergo any surgical intervention or anesthesia.

Controlled cortical impact (CCI)

A craniotomy (4 mm diameter) was made over the right parietal cortex between the sutures of bregma and lambda using a dental drill. The cortical contusion was delivered by a 2.5 mm diameter piston set to an impact depth of 0.5 mm from a pneumatically driven CCI device (VCU Biomedical Engineering Facility, Richmond, VA, USA). The velocity of the piston was set to 2.8 m/s. The bone fragment was put back in place, secured with tissue adhesive (Histoacryl, Braun, Germany), and the scalp was sutured.

Midline fluid percussion injury (mFPI)

A 3 mm-diameter craniotomy was performed, centered at the midline halfway between bregma and lambda, leaving the underlying dura intact. A plastic cap was secured over the craniotomy with dental cement (Heraeus Kulzer, Hanau, Germany). Injury was produced by attaching the saline filled cap to the Luer-Lok fitting on the fluid percussion device (VCU Biomedical Engineering Facility, Richmond, VA, USA) and releasing a pendulum hitting a saline-filled reservoir, producing moderate injury, into the closed cranial cavity. The peak pressure pulse was 1.40 ± 0.06 atm, measured by a transducer displayed on an oscilloscope and recorded on a computer. Immediately after the injury, each mouse was visually monitored for apnea duration and seizures. Anesthesia was then resumed, the cement and the cap were removed, the bone flap was replaced, and the skin was closed with sutures. Mice were moved to a cage with a heating pad until they had recovered from anesthesia and were fully ambulatory.

Morris water maze

To evaluate spatial learning and memory, we used the MWM test [23], in which the mice are placed in white 1.4 m-diameter circular tank, filled 20 cm with 22°C water. The test is performed by putting the mice into different starting positions from where they have to find a fixed 10 cm-diameter platform placed in the southwest quadrant of the tank and submerged 1 cm below the surface. Simple visual cues to aid navigation are placed on roller curtains surrounding the tank. 16 training trials over a 4-day interval (4 trials per day) were performed in the MWM at week 12 or week 24 post-injury. Each swim trial was performed by placing the mouse in the tank at one of four designated entry points facing the wall. The trial was recorded using a digital tracking system (HVS Image, Buckingham, UK). The trial was terminated when the mouse located and stayed on the platform. The mouse was allowed to remain undisturbed on the platform for 15 s or placed there if it had not located the platform in order to acquire the visual cues surrounding the pool. For each MWM learning trial, the latency to find the platform, swim speed and path length were analyzed.

PET scanning

To investigate the *in vivo* brain accumulation of Aβ aggregates, PET scanning was performed with the Aβ protofibril selective antibody-based radioligand [^{124}I]RmAb158-scFv8D3 [24] in mice ($n = 7$ uninjured, $n = 5$ CCI, $n = 7$ mFPI) 24 weeks after TBI. Animals were i.v. administered with 8.7 ± 1.2 MBq [^{124}I]RmAb158-Scfv8D3 3 days prior to PET/CT imaging. PET scanning, 60 min, was conducted under 1.5–2.0% isoflurane anesthesia (Baxter Medical AB, Kista, Sweden) in a Triumph Trimodality System (TriFoil Imaging, Inc., Northridge, CA, USA) followed by a 2 min CT scan obtained in the same scanner. Image reconstruction and analysis of radioligand accumulation in the brain was performed as previously described [25]. All animals were euthanized directly after scanning.

Mouse brain homogenization and fixation

At the time of euthanization, mice were anesthetized with 2.7–3.2% isoflurane (Baxter Medical

AB, Kista, Sweden) followed by intracardiac perfusion with 50 ml physiological saline during 2 min. The brain was removed from the cranium and divided coronally in two parts, just anterior to the brain injury site. The anterior part was snap frozen on dry ice to be used for biochemical quantification of Aβ. The posterior part was placed in paraformaldehyde for 24 h. After 24 h, it was cryoprotected in sucrose (10%, 20%, and finally 30%) and stored in 30% sucrose at 4°C until cryostate-sectioned coronally at a thickness of 14 μm for immunohistochemical analysis.

The anterior tissue was extracted by adding 5 μl cold TBS/mg tissue weight (20 mmol/L Tris and 137 mmol/L NaCl, pH 7.6, complete protease inhibitor cocktail (Roche)). A tissue grinder with Teflon pestle were used with 2 × 10 strokes on ice. The TBS homogenate was mixed with concentrated formic acid to a concentration of 70%, followed by homogenization and centrifugation at 16 000×g at 4°C for 60 min, and the supernatants were stored at –70°C prior to analysis. The reason for mixing TBS with concentrated formic acid to a concentration of 70% is to completely dissolve the tissue and obtain a brain preparation of total Aβ, i.e., including plaque Aβ.

ELISA

Levels of $A\beta_{40}$ and $A\beta_{42}$, corresponding to total Aβ load, was measured in the formic acid (FA) treated brain homogenates, as previously described [25]. In brief, 96-well plates were coated overnight with 100 ng/well of rabbit polyclonal anti-$A\beta_{40}$ or anti-$A\beta_{42}$ (custom made by Agrisera) and blocked with 1% BSA in PBS. FA extracts from frontal cortex were neutralized with 2 M tris and diluted 2000× for $A\beta_{40}$ and 200× for $A\beta_{42}$ analysis, then incubated overnight, followed by detection with biotinylated mAb1C3 (0.5 μg/ml) [26] and streptavidin-HRP (Mabtech AB). Signals were developed with K Blue Aqueous TMB substrate (Neogen Corp.) and read with a spectrophotometer at 450 nm. All dilutions were made in ELISA incubation buffer (PBS with 0.1% BSA, 0.05% Tween20 and 0.15% Kathon).

Immunohistochemistry

Immunohistochemistry was performed on sections localized right before the injury area; Bregma: 1.32–0.38, to evaluate the expression of Aβ, GFAP, Vimentin, Iba-1, Mac-2, MAP-2, synaptophysin and double cortin (DCX) in brain tissue sections from mice at 12- and 24-weeks post injury. All steps were performed at room temperature unless otherwise mentioned. The slides were air dried for 3 min before rehydration in PBS for 5 min. Non-specific binding was blocked with 5% normal goat serum (NGS, Bionordica) in phosphate buffered saline (PBS) + 0.3% Triton X-100 for permeabilization for one hour in a humidity chamber. The blocking buffer was poured off from the slides before incubating with primary antibody, diluted with 0.5% NGS in PBS + 0.03% Triton X-100, in humidity chamber overnight at 4°C. For specific antibodies and dilutions, see Table 1. The slides were washed 3 × 10 min in PBS before incubation with secondary antibody (Table 1), diluted with 0.5% NGS in PBS 0.03% Triton X-100, in humidity chamber at 37°C for 1 h. After washing 3 × 10 min in PBS, slides were mounted with Vectashield Hard Set™ Mounting medium with DAPI (Vector), staining the nuclei.

Quantification and statistics

Morris water maze

Two-way ANOVA was performed for injury group and trial day. Bonferroni's *post-hoc* test was used to describe the differences between the groups (Statistica, Statsoft, Sweden).

PET

Radioligand accumulation was quantified as concentration of [^{124}I]RmAb158-scFv8D3 in frontal cortex relative to that in cerebellum, i.e., a region largely spared of pathology at this age in tg-ArcSwe mice [25, 27]. Thus, the concentration ratio indicates radioligand accumulation above what is expected in normal pathology-free tissue. The concentration ratio, often denoted SUVR, is a standard read-out in preclinical as well as in clinical PET studies. The PET data was analyzed with one-way ANOVA followed by Bonferroni's *post hoc* test and presented as mean ± standard error of the mean (SEM). Significance levels indicated in the figures correspond to: $^{*}p$-value <0.05, $^{**}p$-value <0.01.

ELISA

Aβ concentrations were calculated from a standard curve of serially diluted synthetic $A\beta_{40}$ and $A\beta_{42}$, using a four-parameter equation. The ELISA data was analyzed with one-way ANOVA followed by Bonferroni's *post hoc* test and presented as mean ± standard error of the mean (SEM). Significance levels

Table 1
Overview of antibodies used for immunohistochemistry

Antibody	Host/Dilution	Target	Supplier/product number
Anti-Aβ_{1-16} (6E10)	Mouse, 1:500	Aβ/AβPP	Covance, SIG-39320
Anti-Aβ_{1-16} (82E1)	Mouse, 1:100	Aβ N-terminus	IBL International, JP10323
Anti-DCX	Guinea pig, 1:800	Newborn neurons	Millipore, AB2253
Anti-GFAP	Mouse, 1:400	Reactive astrocytes	DAKO, Z0334
Anti-Iba1	Rabbit, 1:200	Microglia	Wako, 019-19741
Anti-Mac2	Rat, 1:200	Microglia/macrophages	Cedarlane, CL8942AP
Anti-Map2	Rabbit, 1:200	Neurons	Millipore, AB5622
Anti-Synaptophysin	Rabbit, 1:500	Presynaptic marker	Abcam, ab32127
Anti-Vimentin	Chicken, 1:500	Reactive astrocytes	Millipore, AB5733
Anti-chicken 488	Goat, 1:200	Secondary antibody	Thermo Fisher, A11039
Anti-guinea pig 488	Goat, 1:200	Secondary antibody	Thermo Fisher, A11073
Anti-mouse 488	Goat, 1:200	Secondary antibody	Thermo Fisher, A11001
Anti-mouse 555	Goat, 1:200	Secondary antibody	Thermo Fisher, A21424
Anti-rat 488	Goat, 1:200	Secondary antibody	Thermo Fisher, A11006
Anti-rabbit 488	Goat, 1:200	Secondary antibody	Thermo Fisher, A11008
Anti-rabbit 555	Goat, 1:200	Secondary antibody	Thermo Fisher, A21428

indicated in the figures correspond to: $^{*}p$-value <0.05, $^{**}p$-value <0.01.

Immunohistochemistry

The stained brain sections were visualized in a Zeiss Observer Z.1 microscope (Carl Zeiss Microimaging GmbH, Jena, Germany) with objectives 20×/0.4 W, 40×/0.75 W, and 63×/1.4 oil immersion. Images were captured of the regions of interest (ROI) (Supplementary Figure 1B) and the intensity was measured with Zeiss Zen software. For each animal, 3 sections were stained and 10 images/section for cortex and 2 images/section for hippocampus were captured. The data was analyzed by nonparametric Mann Whitney test, using GraphPad Prism (version 5.03) and shown as mean ± standard error of the mean (SEM). Significance levels indicated in the figures correspond to: $^{*}p$-value <0.05, $^{**}p$-value <0.01, and $^{***}p$-value <0.001.

RESULTS

Memory deficits in tg-ArcSwe subjected to TBI

To investigate if CCI or mFPI results in long-term negative effects on spatial learning in tg-ArcSwe mice, we performed MWM analysis at 12 and 24 weeks following the injury and compared their performance to age-matched uninjured tg-ArcSwe mice. At both time points, we found a significant increase in the latency to find the platform ($p < 0.05$) in mice that received TBI, as compared to the uninjured tg-ArcSwe mice (Fig. 1A, B). At the later time point, the mFPI mice performed worse than the CCI mice (Fig. 1B). We did not detect any difference in swim speed between the groups, but the swim distance was significantly increased for the injured mice at 24-weeks post-TBI, compared to uninjured mice, corresponding to the increased latency to find the platform (Supplementary Figure 2).

PET analysis shows earlier Aβ pathology following TBI

PET imaging revealed significantly higher accumulation of [^{124}I]RmAb158-scFv8D3 in the frontal cortex of mFPI and CCI tg-ArcSwe mice, compared to uninjured tg-ArcSwe mice, indicating an increased accumulation of Aβ in this region (Fig. 2A, B). Quantification of total Aβ levels in brain tissue homogenates showed no significant increase in the TBI groups, compared to tg-ArcSwe uninjured mice (Fig. 2C). While this difference was not significant due to high variability, mainly caused by two individuals with very high Aβ load in the mFPI group, there was an overall good correlation with the PET quantification (Fig. 2D).

Increased Aβ deposits and reactive astrocytes 24 weeks following TBI

In order to study the long-term glial response and Aβ pathology in tg-ArcSwe mice following CCI or mFPI, we performed immunohistochemistry with brain sections from animals sacrificed 12 weeks and 24 weeks after the injury. Immunostainings with antibodies specific to the astrocyte marker GFAP, revealed that there was no significant increase in

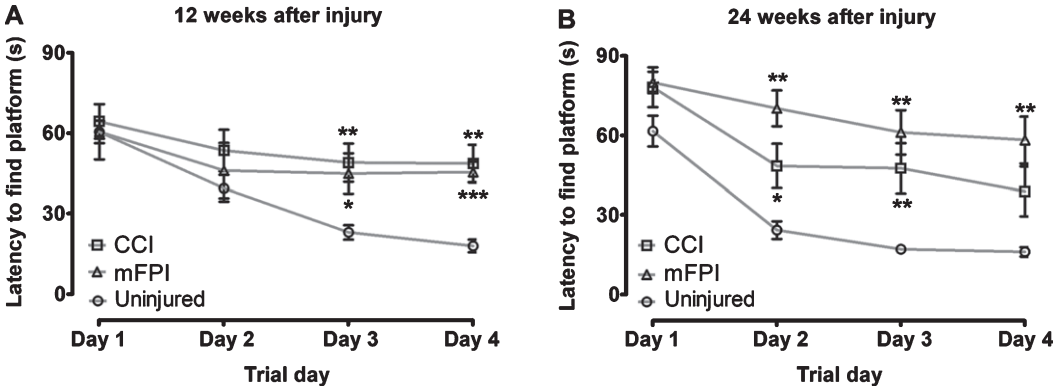

Fig. 1. Severe long-term defects in spatial learning in tg-ArcSwe mice following TBI. The tg-ArcSwe mice performed significantly worse in the Morris water maze test, compared to age-matched uninjured tg-ArcSwe mice at both 12-weeks (A) and 24-weeks (B) post-injury. At the later time point, the mice that had received mFPI mice performed worse than the mice that had received CCI. Two-way ANOVA was performed for injury group and trial day. Bonferroni's *post-hoc* test was used to describe the differences between the groups.

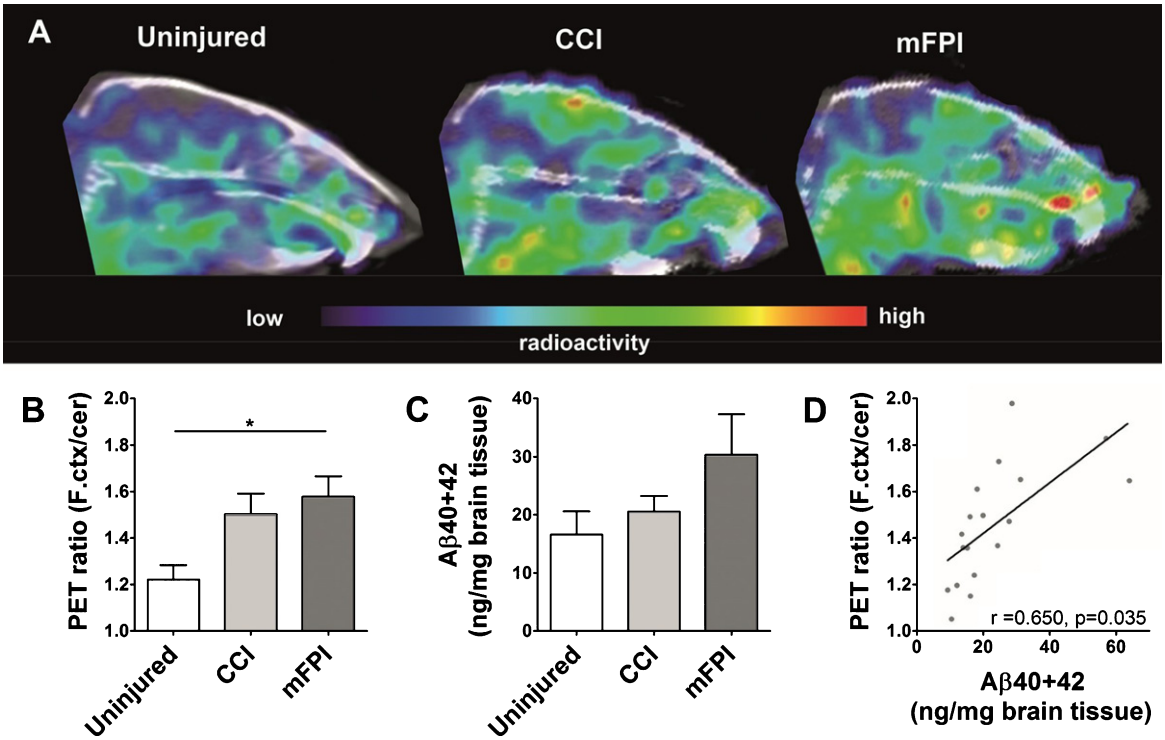

Fig. 2. Earlier Aβ pathology following TBI. Sagittal view of PET images obtained with [^{124}I]RmAb158-scFv8D3 administered to mice 3 days before scanning (A). Quantification of PET ratio (frontal cortex/cerebellum) from PET images revealed that frontal cortex signal was significantly higher in mice subjected to both forms of TBI compared to uninjured mice (B). ELISA Quantification of total total Aβ40 + 42 in frontal cortex showed a similar trend as PET (C), with a significant correlation to the PET ratio (D). The PET data and the ELISA data were analyzed with one-way ANOVA followed by Bonferroni's *post hoc* test. Graphs display group mean with error bars for SEM. *$p < 0.05$; **$p < 0.01$.

GFAP expression 12 weeks after injury (Fig. 3A, B). Instead, there was lower GFAP expression in mice that received mFPI, compared to uninjured animals, while there was no difference between animals that revived CCI and uninjured animals. Interestingly, there was a two-fold increase in GFAP-expression in both groups of injured mice at 24 weeks, compared to uninjured controls. These results indicate a prominent long-term effect of TBI, resulting in a pronounced chronic astroglial response half a year

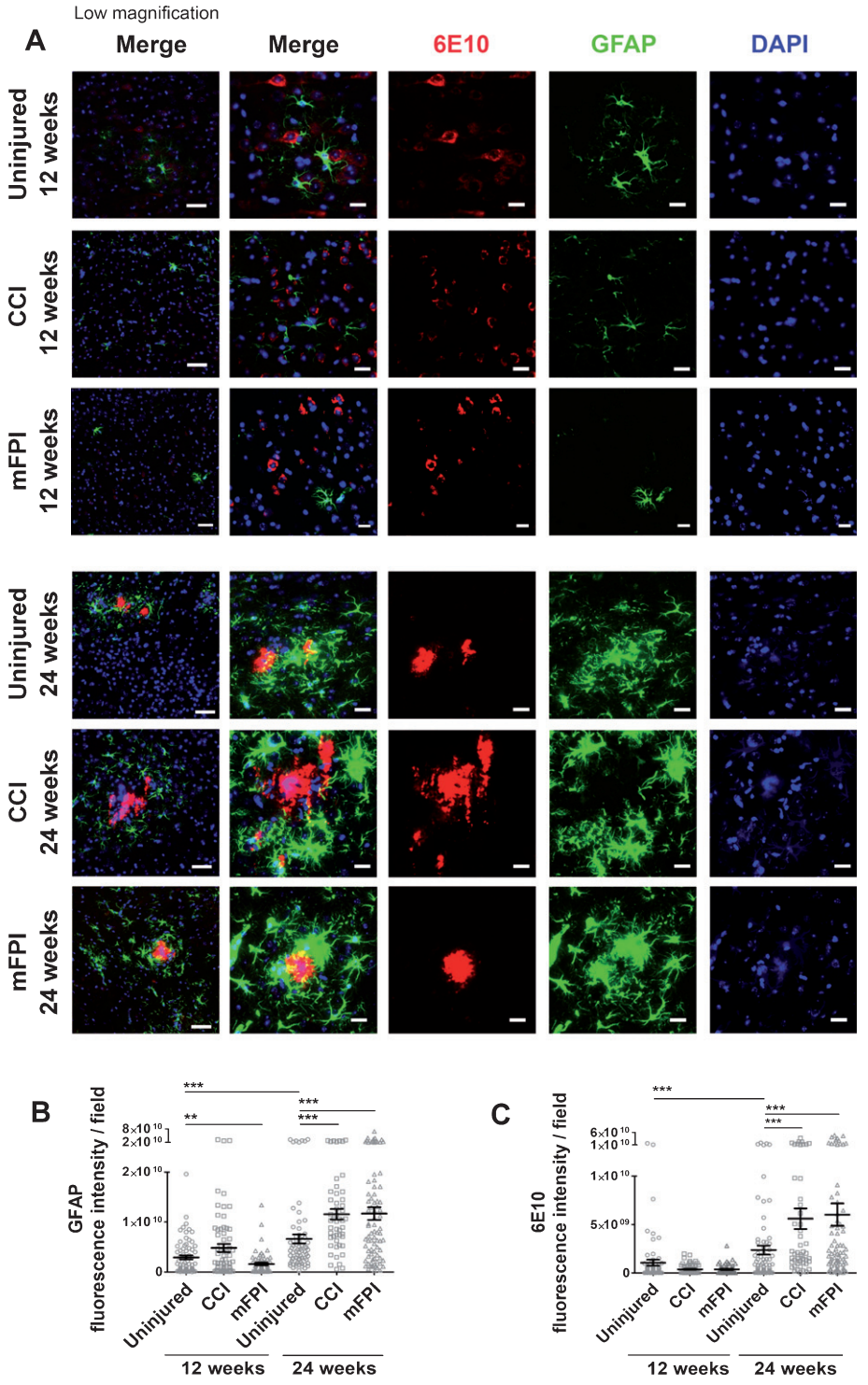

Fig. 3. Elevated GFAP expression and Aβ deposition at 24 weeks following CCI or mFPI. Immunostainings, revealed that there was no significant increase in reactive astrocytes, GFAP (green) and Aβ deposits (6E10, red) in tg-ArcSwe mice at 12 weeks after CCI or mFPI. At24 weeks, there was a clear increase in both GFAP-expression and Aβ deposition in both injury groups at, compared to uninjured controls (A). Analysis of the fluorescence signal confirmed that there was a significant increase in GFAP-expression and Aβ deposition 24 weeks after CCI or mFPI (B-C). The data was analyzed by nonparametric Mann Whitney test and the graphs display mean ± SEM. Scale bars: Low magnification = 20 μm, high magnification = 50 μm. $^{**}p < 0.01$, $^{***}p < 0.001$.

after the trauma. The analysis of Aβ burden in mice, following CCI or mFPI, using the Aβ specific antibody 6E10, confirmed PET and ELISA analyses and demonstrated that both injuries resulted in an increased Aβ pathology as compared to uninjured mice at 24-weeks, but not at 12-weeks post-injury, which is in line with the astrocyte response. Moreover, the immunostainings illustrate that the reactive astrocytes were mostly situated around Aβ plaques (Fig. 3A, C).

Next, we performed additional stainings with specific antibodies to vimentin, a protein that is highly expressed in reactive astrocytes. As predicted, there was a very low expression of vimentin in the uninjured tg-ArcSwe brain. Following CCI, the vimentin expression was markedly induced and could easily be detected (Fig. 4). At 12-weeks post-injury, vimentin was prominently expressed in astrocytes that were in close proximity to the injury-site. However, vimentin expression could not be detected in regions distant from the CCI injury-site or in the brains of mice that received mFPI at this time point. At week 24 after injury, the pattern of vimentin expression was different. Vimentin positive, reactive astrocytes were then frequently found in both injured and uninjured animals, but exclusively around the plaques where it overlapped with GFAP expression (Fig. 4). However, at this time point vimentin expression was very sparse in the region close the CCI lesion site.

Increased number of activated microglia 24 weeks after CCI

In order to analyze the microglia activity in the tg-ArcSwe mouse brain following CCI or mFPI, we performed stainings with antibodies specific for Iba-1 (Fig. 5A, B). At the earlier time point, 12-weeks post-TBI, there was a very sparse expression of Iba-1 in both uninjured and injured mice. Interestingly, there was significantly less Iba-1 expressing microglia in mice that received CCI or mFPI at this time point, compared to uninjured controls (Fig. 5B). At 24 weeks after TBI, there was a two-fold increase of Iba-1 reactivity in mice that received CCI, compared to uninjured tg-ArcSwe mice, indicating that similar to astrocytes, microglia are activated at late time points following injury (Fig. 5B). Notably, CCI resulted in a more prominent late microglial activation, compared to mFPI. Double stainings with the Aβ antibody 82E1 clearly demonstrated that microglia were predominately found in close proximity to the plaques (Fig. 5A).

Next, we examined the number of activated, Mac-2 positive microglia/macrophages in the in tg-ArcSwe mouse brain 12 and 24 weeks following CCI or mFPI (Fig. 6). There was a very low number of Mac-2 positive cells in both uninjured and injured mice. At the later time point, Mac-2 positive cells were found around the plaques of both uninjured and injured mice. However, the Mac-2 staining was strongest in CCI-injured animals at both time points (Fig. 6). Quantification of the Mac-2 positive cells revealed 0.4 ± 0.7 positive cells/field in uninjured animals, 10.9 ± 5.0 positive cells/field in CCI-mice and 1.9 ± 2.6 positive cells/field in mFPI-mice at 12 weeks. At 24 weeks there was 2.1 ± 1.0 positive cells/field in uninjured animals, 11.5 ± 6.1 positive cells/field in CCI-mice, and 2.7 ± 1.9 positive cells/field in mFPI-mice.

Elevated expression of synaptophysin 24 weeks after TBI

In our investigation of cellular processes that could be altered by CCI or mFPI, we next studied the neuronal dendrite network in tg-ArcSwe mouse brain following CCI or mFPI, by using specific antibodies to MAP2 (Fig. 7). Our immunostainings showed that there was a clear disruption of the MAP2 positive processes in the areas of Aβ pathology at the 24-week time point that was not seen at week 12. Where the plaques had developed, there were clear gaps in the MAP2-staining. However, no obvious differences between uninjured mice and mice that received CCI or mFPI was observed and around the plaques, the dendrite network appeared intact (Fig. 7).

Synapse alterations are widespread in AD and we therefore sought to investigate the effect of CCI and mFPI on the synapse specific marker synaptophysin in the region of hippocampus (Fig. 8A, B). Immunocytochemistry demonstrated that there was no significant difference in synaptophysin expression at 12 weeks following TBI, as compared to uninjured controls. However, at the later time point, 24 weeks post-injury, there was a clear increase in synaptophysin expression in both the CCI and mFPI animals, indicating a possible compensatory effect due to synaptic dysfunction (Fig. 8B).

Increased cell loss in hippocampus at later time points following TBI

It is well-known that TBI, as well as early AD pathology, could stimulate neurogenesis [28, 29].

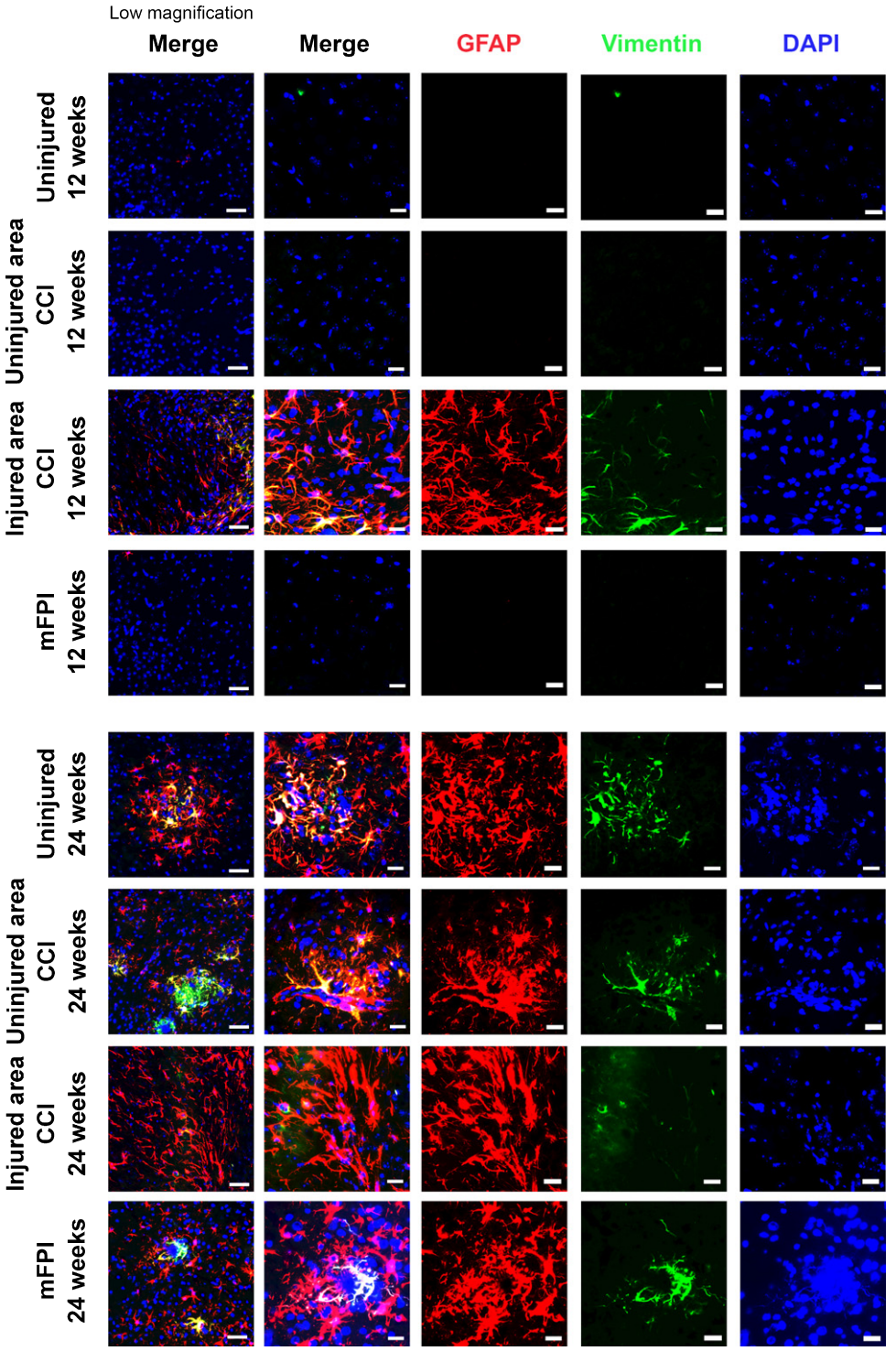

Fig. 4. Increased expression of Vimentin at 12 weeks following CCI. Immunostainings demonstrated that Vimentin (red) and GFAP (green) had different expression patterns. There was a clear increase of Vimentin positive astrocytes in close proximity to the lesion site at 12 weeks following CCI (injured area CCI), while the expression in distant regions was very low. At week 24, Vimentin positive astrocytes were frequently found in both injured and uninjured animals, but exclusively around the plaques where the Vimentin expression overlapped with the GFAP expression. The Vimentin expression close to the CCI lesion site was very sparse at this time point. Scale bars: Low magnification = 20 μm, high magnification = 50 μm.

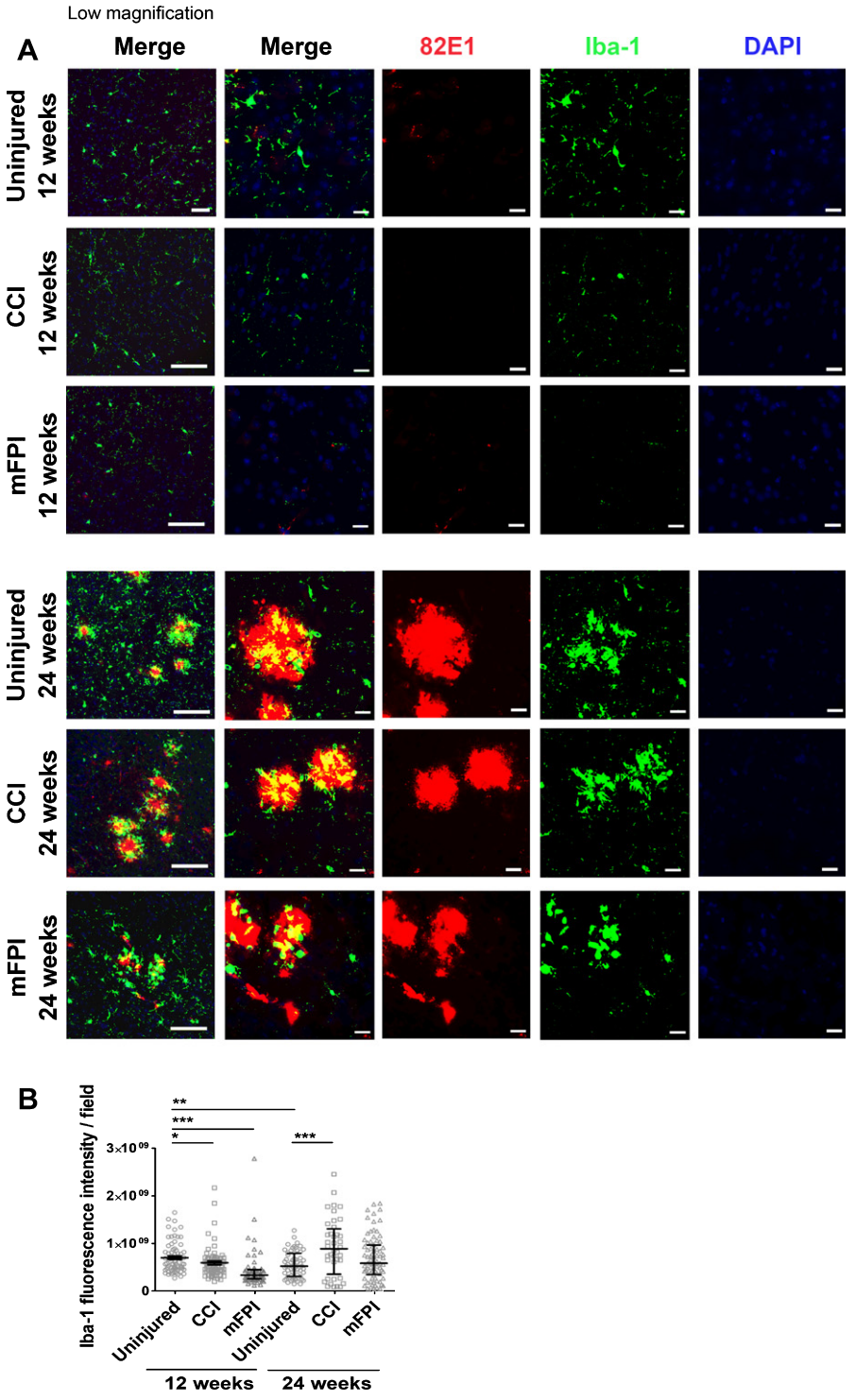

Fig. 5. Induced number of activated microglia 24 weeks after CCI. Immunostainings with antibodies specific for Iba-1 (green) and the Aβ antibody 82E1 (red) demonstrated that microglia were found in close proximity to the plaques (A). At 12-weeks post-TBI there was a sparse expression of Iba-1 in both uninjured and injured mice. There was significantly less Iba-1 expression in mice that received CCI or mFPI at this time point, compared to uninjured controls. 24 weeks after TBI there was a two-fold increase of Iba-1 reactivity in mice that received CCI, compared to uninjured tg-ArcSwe mice (B). The data was analyzed by nonparametric Mann Whitney test and the graph displays mean ± SEM. Scale bars: Low magnification = 20 μm, high magnification = 50 μm. *$p < 0.05$, **$p < 0.01$, ***$p < 0.001$.

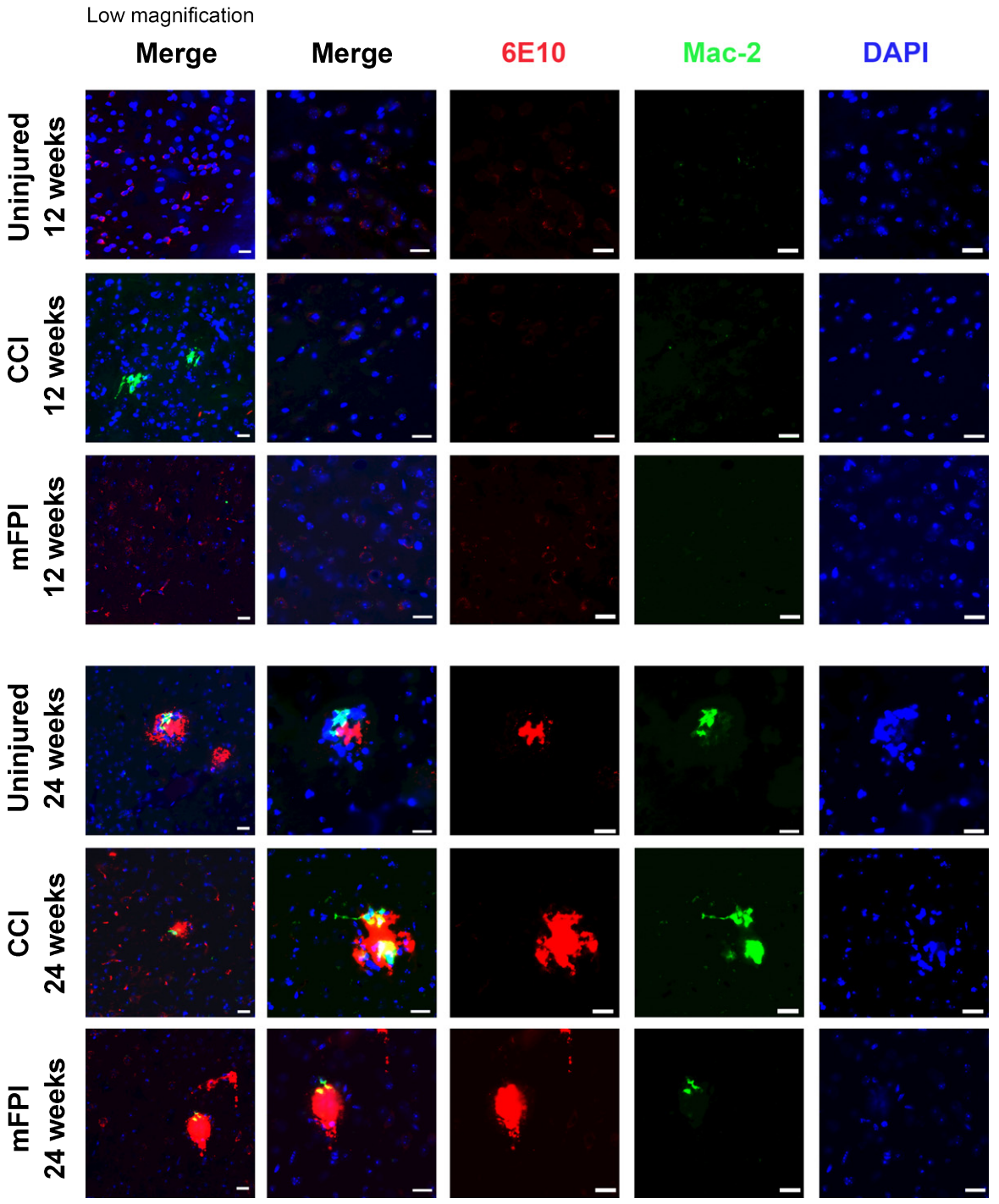

Fig. 6. Mac-2 positive cells around plaques in both uninjured and injured mice. Immunostainings using specific antibodies to amyloid-β (6E10, red) and activated microglia/macrophages (Mac-2, green) showed that there was a very low number of Mac-2 positive cells in the brains of both uninjured and injured mice at 12 weeks post-injury. At 24 weeks post-injury, there was an increased number of Mac-2 positive cells found around the plaques of both uninjured and injured mice, but the Mac-2 staining was strongest in CCI-injured animals. Scale bars: 20 μm.

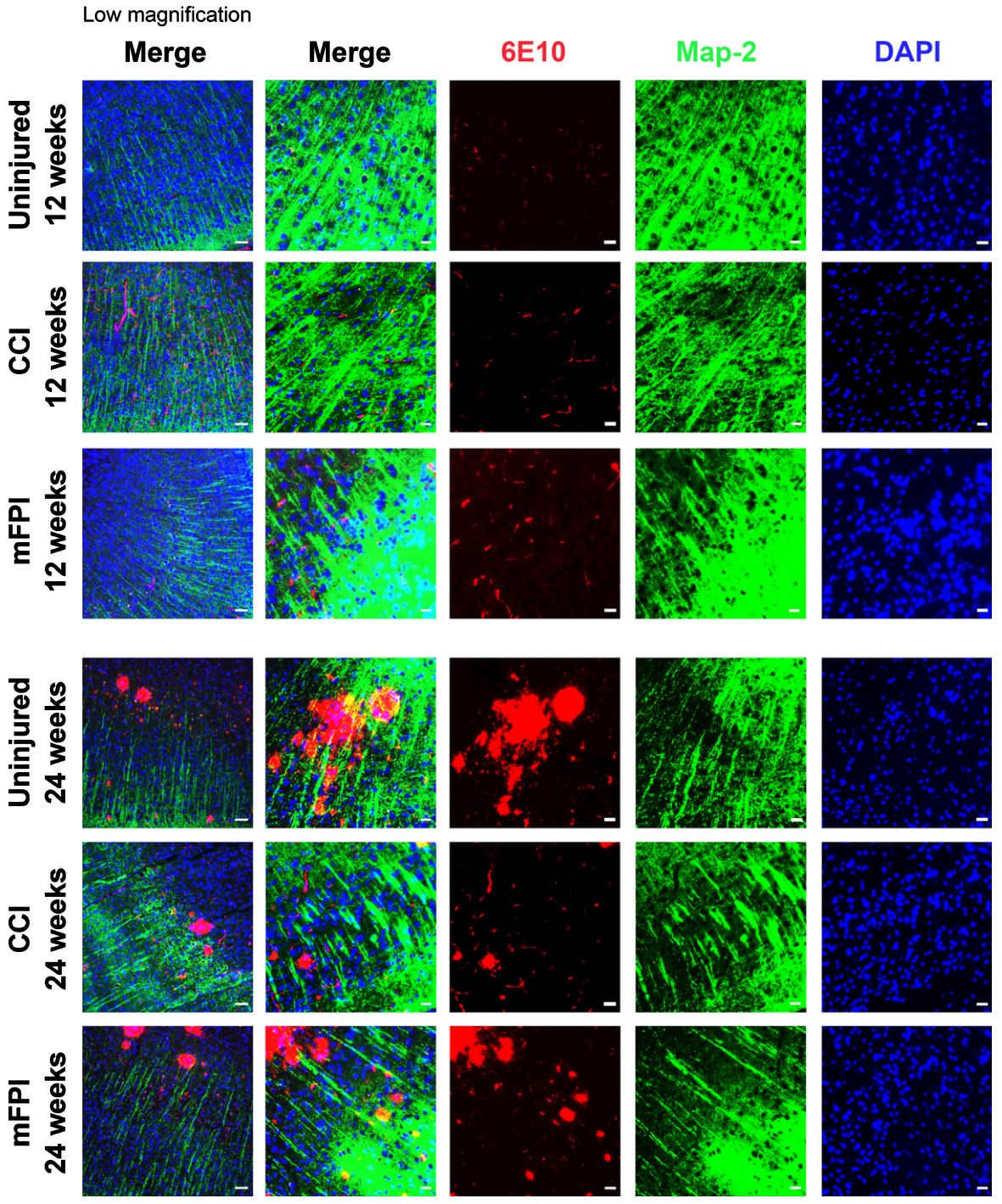

Fig. 7. Aβ pathology interrupts neuronal processes in older animals. Immunocytochemistry showed that there is a clear disruption of the MAP2 positive (green) neuronal processes in the areas of Aβ pathology (6E10, red), especially at the 24-week time point. Scale bars: Low magnification = 20 μm, high magnification = 50 μm.

Therefore, we analyzed the number of DCX positive neuroblasts in the tg-ArcSwe mouse brain following CCI or mFPI (Fig. 9A, B). We found newly formed neuroblasts in all mice at both time points, but there were fewer DCX positive cells at the later time point in both uninjured and injured animals. However, the

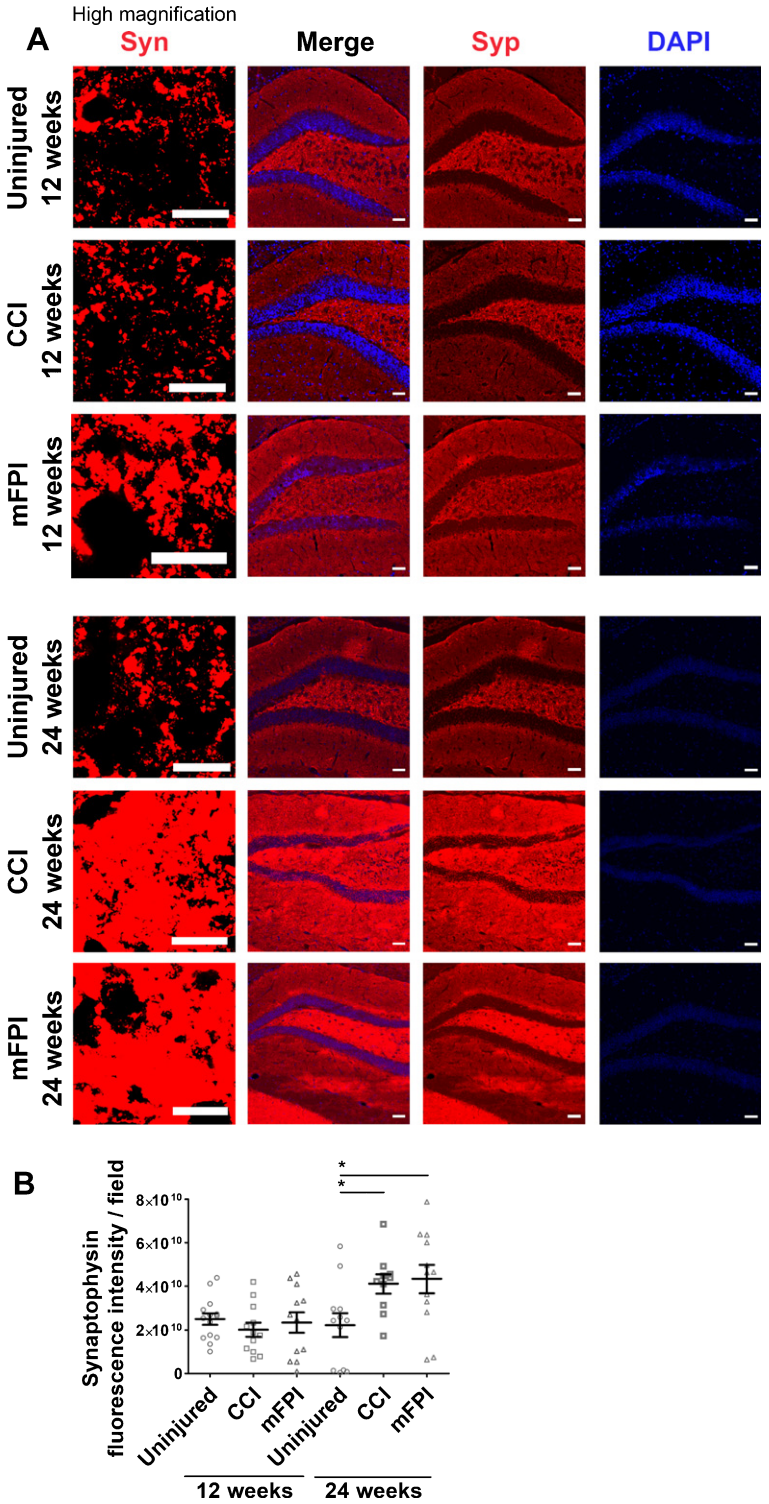

Fig. 8. Elevated expression of synaptophysin 24 weeks after TBI. Immunocytochemistry (A) followed by analysis of the fluorescence signal (B) demonstrated that there was no significant difference in synaptophysin (Syn, red) expression at 12 weeks following TBI, as compared to uninjured controls. At 24-weeks post-injury, it was a clear increase in synaptophysin expression in both the CCI and mFPI animals. The data was analyzed by nonparametric Mann Whitney test and the graph displays mean ± SEM. Scale bars: Low magnification = 10 μm, high magnification = 50 μm. $*p < 0.05$.

TBI had no significant impact on the number of newly formed neuroblasts at these time points (Fig. 9B).

In order to investigate the effect of CCI and mFPI on hippocampal cell loss, we analyzed the cell number by labelling the cell nuclei with DAPI (Fig. 10A–C). Measurements of the hippocampus thickness revealed a significant reduction at 12-weeks post-TBI in mice that received CCI or mFPI, compared to uninjured controls (Fig. 10B). At the later time point, 24 weeks, the hippocampus were reduced in all animal groups and there was no longer any difference between uninjured and injured mice (Fig. 10B). A significant decline in the number of DAPI stained nuclei per area was also found in the CCI and mFPI animals at 12-weeks post-TBI (Fig. 10C). For the mFPI animals, the DAPI stained nuclei per area was still significantly lower than the uninjured animals at 24-weeks post-injury (Fig. 10C).

DISCUSSION

TBI is one of the leading causes of death and disability worldwide. In addition, it is known from epidemiological studies that moderate to severe TBI constitutes a risk factor for AD. Brain trauma induces multiple acute and chronic changes in the brain, for example oxidative stress, axonal degeneration, vascular damage, and widespread neuroinflammation [30]. However, the exact mechanism behind the increased risk to develop AD remains elusive.

The aim with the present study was to identify cellular processes that could link TBI to AD development, by investigating the chronic impact of two different injury models, controlled cortical impact (CCI) and midline fluid percussion injury (mFPI). It is important to remember that cellular events in animal models of AD and TBI may or may not reflect the disease processes in the human brain. In the human situation, the trauma often occurs years before AD onset. However, to mimic the disease process in a mouse model, the time line had to be adjusted. To study the effect of TBI on AD initiation and progression, it was important to induce the trauma before the mice show any visible Aβ pathology. Hence, 3 months was a good time point. The first investigated time point, when animals were 6 months old (12 weeks following TBI), coincides with the very first appearance of plaques in uninjured tg-ArcSwe mice and the second time point, when the animals were 9 months old (24 weeks following TBI), coincides with pronounced Aβ pathology in uninjured tg-ArcSwe mice. The long-term effect of the TBI on memory deficiency, Aβ pathology, neurodegeneration, and inflammation was investigated by MWM, PET imaging, immunohistochemistry, and biochemical analyses.

Our results from the MWM analysis demonstrate that mice that received CCI or mFPI performed significantly worse than uninjured tg-ArcSwe mice, especially at the later time point, which corresponds to an increased Aβ accumulation. Interestingly, we found that at the later time point, the mFPI mice performed worse than the CCI mice. A possible explanation for this could be that the diffuse injury induced by mFPI progresses more severely over time, compared to the more focal injury induced by CCI. The diffuse injury affects the white matter and axons to a much larger extent than the focal injury, and it is possible that the amyloid protein accumulation causes more cognitive deficits over time in this scenario compared to the more encapsulated focal injury caused by CCI. In a recent study, using a novel technique of tissue preparation, it was found that many axonal swellings after CCI probably were not as severe as reported earlier in the literature. This could suggest that the progression after CCI is rather slow [31]. In another strain of AD-mice (APP-PS1), it has been reported that young mice develop more post-TBI problems than older mice [32].

AD is characterized by key neuropathological features, including extracellular accumulation of Aβ in plaques, intracellular aggregation of microtubule-associated protein tau in neurofibrillary tangles and neuroinflammation. According to the amyloid cascade hypothesis, Aβ is the causative agent of AD, consequently driving the formation of neurofibrillary tangles, vascular damage, inflammation, and neuronal cell loss [2, 33]. Accumulation of Aβ in the AD brain is caused by an imbalance between Aβ production and Aβ clearance and mutations in amyloid-β protein precursor (AβPP) are known to result in early-onset AD by increasing the Aβ levels [34]. However, since the majority of patients with late-onset AD do not have an increased Aβ production, it has been suggested that the main cause of this form of the disease is instead insufficient lysosomal degradation [35, 36] or other factors resulting in increased cellular stress, such as oxidative stress, inflammation, or bacterial infections, which in turn result in the accumulation of aggregated proteins [5, 33].

Importantly, both Aβ and neurofibrillary changes begin during preclinical AD when cognitive deficits are not apparent [37]. It was shown in the present

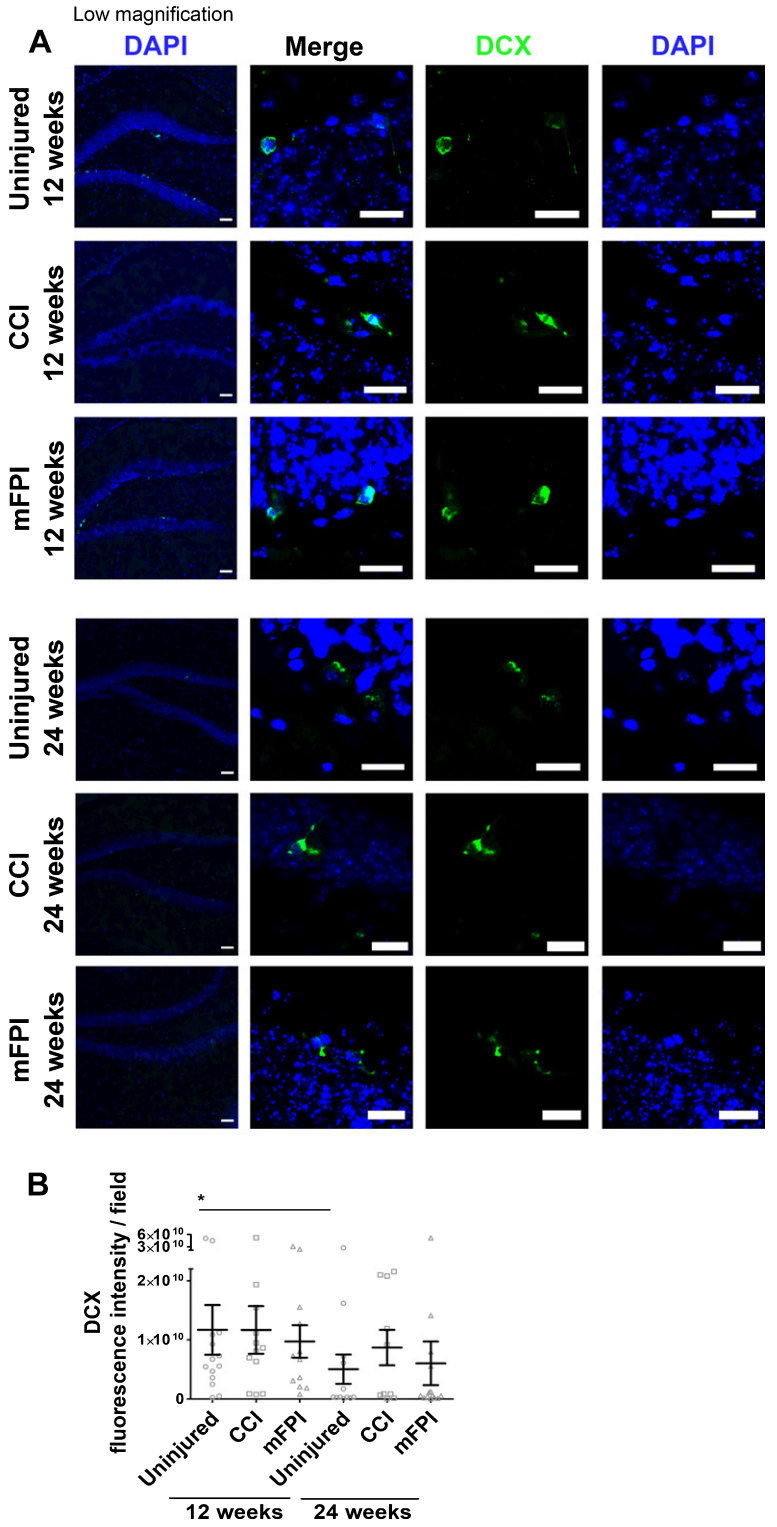

Fig. 9. No effect on neurogenesis 12 and 24 weeks after TBI. Immunohistochemistry demonstrated that double cortin (DCX, green) positive neuroblasts were present in the tg-ArcSwe mouse brain following CCI or mFPI and in uninjured controls (A). There was fewer DCX positive cells at the later time point in both uninjured and injured animals (B). The data was analyzed by nonparametric Mann Whitney test and the graph displays mean ± SEM. Scale bars: Low magnification = 20 μm, high magnification = 50 μm. *$p < 0.05$.

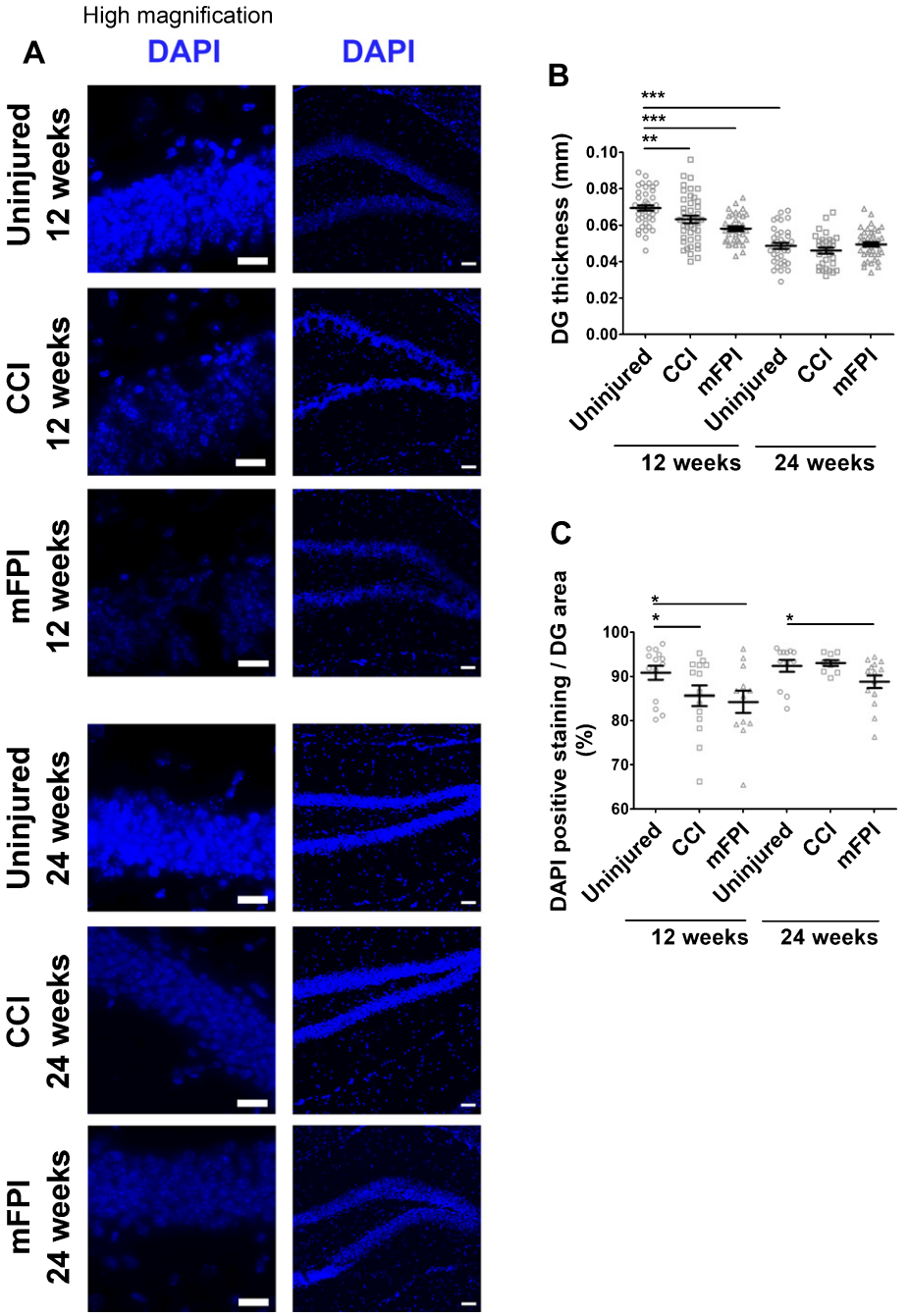

Fig. 10. Increased cell loss in hippocampus at 24 weeks following TBI. The nuclei of the cells were labelled with DAPI (A). There was a significant reduction in hippocampal thickness in both injury group at 12 weeks, as compared to uninjured tg-ArcSwe mice. At 24 weeks, the hippocampal thickness was reduced in all animal groups (B). The DAPI stained nuclei per area was also reduced in the CCI animals at 12 weeks and the mFPI animals at 12 and 24 weeks (C). The data was analyzed by nonparametric Mann Whitney test and the graphs display mean ± SEM. Scale bars: Low magnification = 20 μm, high magnification = 50 μm. *$p < 0.05$, **$p < 0.01$, ***$p < 0.001$.

study that TBI caused an earlier formation of Aβ pathology, compared to what is observed in the uninjured tg-ArcSwe brain, and further that Aβ levels could be monitored by PET. Likewise, the emergence of tau PET radioligands [38] might be an aid in the future to monitor *in vivo* changes leading to dementia in the brain after TBI. Interestingly, studies in patients using PET ligands for activated microglia

found abnormal chronic inflammatory response up to 17 years after the TBI event [39], pointing to neuroinflammation as a chronic process which may affect brain function for years after TBI.

Immunohistochemistry analysis of Aβ burden in mice, following CCI or mFPI confirmed PET and ELISA results and demonstrated that both injuries resulted in increased pathology at 24-weeks, but not 12-weeks post-injury. Hence the injury induces a delayed accumulation of Aβ in the brain, several months following TBI. Studies of brain autopsies from young TBI patients who died during the acute phase after injury have demonstrated that Aβ plaques, similar to those found in AD patients, are present at the lesion site shortly after the trauma [40]. It is possible that this acute accumulation of Aβ promotes cellular dysfunction in the brain, i.e., degradation impairment that eventually results in the chronic Aβ pathology. Effective waste removal is crucial for maintaining a healthy brain and any alteration in the clearance capacity may contribute to the development of AD and dementia [41]. We have previously shown that astrocytes ingest large amounts of aggregated Aβ, but then store, rather than degrade the ingested material. The incomplete digestion results in a high intracellular load of neurotoxic Aβ species and severe lysosomal dysfunction [42]. Hence, the Aβ-induced degradation impairments will easily turn into a negative spiral.

Interestingly, the severe memory deficits in tg-ArcSwe mice following TBI could not be explained by synaptic loss. Instead, the synapse marker synaptophysin was increased in TBI mice compared to uninjured controls, indicating a compensatory induction of synaptogenesis. However, it was obvious that the increased synapse formation could not rescue the memory function, indicating that the regenerating synapses might be none-functional. Neuroregenerative processes are known to be induced by trauma or diseases in the brain, but apparently the plasticity cannot effectively compensate for the lost behavioral functions. It is possible that the increased regeneration can even result in adverse effects. For example, sprouting of mossy fibers following TBI has been suggested to result in epilepsy [43–45]. In contrast to the increased synaptogenesis, our quantification of DCX positive cells, showed that there is no long-term effect on neurogenesis following TBI in the tg-ArcSwe mice.

At 24-weeks post-injury, the mFPI mice demonstrated more severe memory deficits than the CCI mice. This result was in line with the long-term decline in the number of DAPI stained nuclei per area in hippocampus following mFPI, compared to uninjured control mice. Since mFPI results in widespread axonal injury throughout the brain, while CCI results in a local ipsilateral cortical contusion [22], there is much evidence that white matter injury is linked to much later cognitive impairment in patients (exhaustively reviewed by Filley and Kelly) [46]. One of the proposed mechanisms is widespread and chronic neuroinflammation [47] and another is an accelerated aging of the brain [48]. It is important to remember that wild type mice recover surprisingly well following TBI. For example, it was recently shown that mice that receive a single TBI perform as well as the uninjured controls in the MWM test at 6-months post-injury. However, repetitive injuries result in long-term memory deficits [49]. It is obvious from our analysis of cell density in the hippocampus that the mice recover rather well from the acute injury.

Carrying *APOE* ε4 is one of the strongest genetic risk factors in developing late-onset AD [50]. Interestingly, recovery from TBI also seem to be influenced by *APOE*. Inducing CCI in PDAPP mice (that develop AD symptoms), expressing human *APOE3*, human *APOE4*, or no *APOE*, indicated that *APOE4* may indeed influence the long-term neurodegenerative cascade after TBI via an effect on Aβ [51].

In this study we demonstrate that TBI resulted in a pronounced chronicastroglial response half a year after the trauma, based on the GFAP expression. Interestingly, there was a two-fold increase in GFAP-expression in both groups of injured mice at 24 weeks, compared to uninjured tg-ArcSwe controls, but there was no significant increase in GFAP expression, at 12 weeks. On the contrary, mice subjected to mFPI had lower GFAP expression 12 weeks after injury, compared to uninjured animals. This is a novel and interesting finding, since at 24 weeks the mFPI-subjected mice showed increased amount of GFAP, suggesting a transient decrease in reactive astrocytes after mFPI. In a more acute study of mild (not midline) FPI in wild type mice, Powell et al. found a peak of GFAP expression 3 days after injury and that the levels had returned to uninjured control levels 21 days after injury [52]. In our own laboratory, we have previously noticed an increase of GFAP-immunoreactivity up to 7 days after injury in wild type mice. However, the signs of a compromised blood-brain barrier peaked at 3 days after injury and decreased until day 7 [53]. This suggests that the mice recover after mild FPI initially. Our

finding in the present study suggest that the diffuse injury in tg-ArcSwe mice may cause a decrease in reactive astrocytes compared to uninjured animals. To fully elucidate this phenomenon will require more research, but hypothetically, an initial stimulation of the astrocytes could result in a downregulation of GFAP-expression temporarily. As the diffuse injury, progresses between 12 and 24 weeks the astrocytes turn more reactive again, as seen in the increased GFAP-immunoreactivity at 24 weeks.

In a previous a study, we have demonstrated that the expression pattern of vimentin and GFAP differ in old tg-ArcSwe mice [54]. In 16-month-old tg-ArcSwe mice, vimentin-positive cells are found distinctly around the plaques, while GFAP-positive cells are found throughout the brain. Many of the reactive astrocytes co-express GFAP and vimentin. Among the cells only express one of the markers, there are more single positive cells for GFAP than for vimentin. Moreover, the expression of vimentin in the wild type mice is much lower than the GFAP expression and vimentin positive cells are only found in the hippocampus and surrounding the ventricles. In the present study we found that the expression of vimentin was markedly induced at 12-weeks post-injury, in astrocytes that were in close proximity to the injury-site. At the later time point vimentin positive, reactive astrocytes were frequently found in both injured and uninjured animals, but exclusively around and not at the injury site. Hence, the timing of the increase of the two markers are different. While the vimentin expression peaks at the earlier time point the expression of GFAP comes later. The explanation for this could be that the markers are expressed at different stages of the chronic inflammation or by different subclasses of astrocytes. For example, a subclass of the reactive astrocytes is known to acquire neural stem cell potential after injury [55]. Our immunostainings show that the vimentin + GFAP + cells were situated tightly around the plaques at the later time point, while vimentin– GFAP + cells were found also in the surrounding tissue. The role of reactive astrocytes in AD development has recently received much attention [56]. Their complex role in the AD brain is thought to depend largely on their release and uptake of substances from the microenvironment that they share with neurons. Being the most abundant glial cell, astrocytes play an important role in maintaining brain homeostasis [57]. Neurodegenerative diseases, including AD, are defined by loss of brain homeostasis, which at least partly could be due to the severely stressed astrocytes that are unable to fulfil their normal tasks [58]. Our previous studies indicate that astrocytes play a central role in the progression of AD, by accumulating and spreading toxic Aβ species [42, 59]. Interestingly, it was recently shown that wild type rats subjected to CCI, displayed several-fold increased MHCII expression as well as accumulation of phosphorylated tau and AβPP 6 months later [60]. Whether the MHCII expressing cells were astrocytes or microglia (or both) were however not studied.

Analysis of the Iba-1 reactivity following TBI in the present study showed that the activation of microglia followed the same pattern as the GFAP+astrocytes, with a two-fold increase of Iba-1 at 24 weeks after TBI. Similar to the GFAP expression there was no significant increase in Iba-1 expression at the earlier time point. Interestingly, CCI resulted in a more prominent late microglial activation, compared to mFPI. Moreover, Mac-2 positive microglia/macrophages were most prominent in the CCI-injured animals at 24 weeks post-injury. Taken together, the immunohistochemistry to glial markers indicate that the chronic inflammation is peaking rather late following injury and that CCI results in a more prominent long-term macrophage/microglial activation, compared to mFPI.

Conclusions

The relationship between TBI and AD is not understood. In the present study, we demonstrate that TBI induces severe memory deficits in a mouse model of AD, several months after the injury. The injured mice showed a late upregulation of reactive gliosis, which concurred with a more pronounced Aβ pathology, compared to uninjured AD mice. Our results suggest that delayed glial activation may occur following TBI. However, further studies in both experimental models and human TBI patients will be required to explore the relationship between this phenomenon and the onset of AD. By answering the question, whether and how TBI contributes to the development of AD later in life, we may also understand the crucial mechanisms of AD development in general.

ACKNOWLEDGMENTS

This study was supported by grants from the Swedish Research Council, the Swedish Alzheimer Foundation, Åhlén Foundation, Hedlund's Foundation, the Swedish Brain Foundation, and the Uppsala Berzelii Center. We are grateful to Lars N.G. Nilsson, who developed and characterized the mouse model.

The molecular imaging work in this study was performed at SciLifeLab Pilot Facility for Preclinical PET-MRI, a Swedish nationally available imaging platform at Uppsala University, Sweden, financed by the Knut and Alice Wallenberg Foundation.

Authors' disclosures available online (https://www.j-alz.com/manuscript-disclosures/19-0572r2).

SUPPLEMENTARY MATERIAL

The supplementary material is available in the electronic version of this article: http://dx.doi.org/10.3233/JAD-190572.

REFERENCES

[1] Kukull WA, Higdon R, Bowen JD, McCormick WC, Teri L, Schellenberg GD, van Belle G, Jolley L, Larson EB (2002) Dementia and Alzheimer disease incidence: A prospective cohort study. *Arch Neurol* **59**, 1737-1746.

[2] Musiek ES, Holtzman DM (2015) Three dimensions of the amyloid hypothesis: Time, space and 'wingmen'. *Nat Neurosci* **18**, 800-806.

[3] Johnson VE, Stewart W, Smith DH (2010) Traumatic brain injury and amyloid-beta pathology: A link to Alzheimer's disease? *Nat Rev Neurosci* **11**, 361-370.

[4] Ramsay RR (1991) Kinetic mechanism of monoamine oxidase A. *Biochemistry* **30**, 4624-4629.

[5] Karran E, De Strooper B (2016) The amyloid cascade hypothesis: Are we poised for success or failure? *J Neurochem* **139** (Suppl 2), 237-252.

[6] Masel BE, DeWitt DS (2010) Traumatic brain injury: A disease process, not an event. *J Neurotrauma* **27**, 1529-1540.

[7] Wilson L, Stewart W, Dams-O'Connor K, Diaz-Arrastia R, Horton L, Menon DK, Polinder S (2017) The chronic and evolving neurological consequences of traumatic brain injury. *Lancet Neurol* **16**, 813-825.

[8] Nonaka M, Chen XH, Pierce JE, Leoni MJ, McIntosh TK, Wolf JA, Smith DH (1999) Prolonged activation of NF-kappaB following traumatic brain injury in rats. *J Neurotrauma* **16**, 1023-1034.

[9] Nakagawa Y, Reed L, Nakamura M, McIntosh TK, Smith DH, Saatman KE, Raghupathi R, Clemens J, Saido TC, Lee VM, Trojanowski JQ (2000) Brain trauma in aged transgenic mice induces regression of established abeta deposits. *Exp Neurol* **163**, 244-252.

[10] Uryu K, Laurer H, McIntosh T, Pratico D, Martinez D, Leight S, Lee VM, Trojanowski JQ (2002) Repetitive mild brain trauma accelerates Abeta deposition, lipid peroxidation, and cognitive impairment in a transgenic mouse model of Alzheimer amyloidosis. *J Neurosci* **22**, 446-454.

[11] Abrahamson EE, Ikonomovic MD, Ciallella JR, Hope CE, Paljug WR, Isanski BA, Flood DG, Clark RS, DeKosky ST (2006) Caspase inhibition therapy abolishes brain trauma-induced increases in Abeta peptide: Implications for clinical outcome. *Exp Neurol* **197**, 437-450.

[12] Laskowitz DT, Song P, Wang H, Mace B, Sullivan PM, Vitek MP, Dawson HN (2010) Traumatic brain injury exacerbates neurodegenerative pathology: Improvement with an apolipoprotein E-based therapeutic. *J Neurotrauma* **27**, 1983-1995.

[13] Schwetye KE, Cirrito JR, Esparza TJ, Mac Donald CL, Holtzman DM, Brody DL (2010) Traumatic brain injury reduces soluble extracellular amyloid-beta in mice: A methodologically novel combined microdialysis-controlled cortical impact study. *Neurobiol Dis* **40**, 555-564.

[14] Tran HT, LaFerla FM, Holtzman DM, Brody DL (2011) Controlled cortical impact traumatic brain injury in 3xTg-AD mice causes acute intra-axonal amyloid-beta accumulation and independently accelerates the development of tau abnormalities. *J Neurosci* **31**, 9513-9525.

[15] Tajiri N, Kellogg SL, Shimizu T, Arendash GW, Borlongan CV (2013) Traumatic brain injury precipitates cognitive impairment and extracellular Abeta aggregation in Alzheimer's disease transgenic mice. *PLoS One* **8**, e78851.

[16] Washington PM, Morffy N, Parsadanian M, Zapple DN, Burns MP (2014) Experimental traumatic brain injury induces rapid aggregation and oligomerization of amyloid-beta in an Alzheimer's disease mouse model. *J Neurotrauma* **31**, 125-134.

[17] Webster SJ, Van Eldik LJ, Watterson DM, Bachstetter AD (2015) Closed head injury in an age-related Alzheimer mouse model leads to an altered neuroinflammatory response and persistent cognitive impairment. *J Neurosci* **35**, 6554-6569.

[18] Cheng WH, Stukas S, Martens KM, Namjoshi DR, Button EB, Wilkinson A, Bashir A, Robert J, Cripton PA, Wellington CL (2018) Age at injury and genotype modify acute inflammatory and neurofilament-light responses to mild CHIMERA traumatic brain injury in wild-type and APP/PS1 mice. *Exp Neurol* **301**, 26-38.

[19] Collins JM, King AE, Woodhouse A, Kirkcaldie MT, Vickers JC (2015) The effect of focal brain injury on beta-amyloid plaque deposition, inflammation and synapses in the APP/PS1 mouse model of Alzheimer's disease. *Exp Neurol* **267**, 219-229.

[20] Philipson O, Lord A, Gumucio A, O'Callaghan P, Lannfelt L, Nilsson LN (2010) Animal models of amyloid-beta-related pathologies in Alzheimer's disease. *FEBS J* **277**, 1389-1409.

[21] Lord A, Kalimo H, Eckman C, Zhang XQ, Lannfelt L, Nilsson LN (2006) The Arctic Alzheimer mutation facilitates early intraneuronal Abeta aggregation and senile plaque formation in transgenic mice. *Neurobiol Aging* **27**, 67-77.

[22] Lifshitz J, Rowe RK, Griffiths DR, Evilsizor MN, Thomas TC, Adelson PD, McIntosh TK (2016) Clinical relevance of midline fluid percussion brain injury: Acute deficits, chronic morbidities and the utility of biomarkers. *Brain Inj* **30**, 1293-1301.

[23] Morris R (1984) Developments of a water-maze procedure for studying spatial learning in the rat. *J Neurosci Methods* **11**, 47-60.

[24] Hultqvist G, Syvanen S, Fang XT, Lannfelt L, Sehlin D (2017) Bivalent brain shuttle increases antibody uptake by monovalent binding to the transferrin receptor. *Theranostics* **7**, 308-318.

[25] Sehlin D, Fang XT, Cato L, Antoni G, Lannfelt L, Syvanen S (2016) Antibody-based PET imaging of amyloid beta in mouse models of Alzheimer's disease. *Nat Commun* **7**, 10759.

[26] Englund H, Sehlin D, Johansson AS, Nilsson LN, Gellerfors P, Paulie S, Lannfelt L, Pettersson FE (2007) Sensitive ELISA detection of amyloid-beta protofibrils in biological samples. *J Neurochem* **103**, 334-345.

[27] Meier SR, Syvanen S, Hultqvist G, Fang XT, Roshanbin S, Lannfelt L, Neumann U, Sehlin D (2018) Antibody-

based *in vivo* PET imaging detects amyloid-beta reduction in Alzheimer transgenic mice after BACE-1 inhibition. *J Nucl Med* **59**, 1885-1891.

[28] Kernie SG, Parent JM (2010) Forebrain neurogenesis after focal Ischemic and traumatic brain injury. *Neurobiol Dis* **37**, 267-274.

[29] Lopez-Toledano MA, Ali Faghihi M, Patel NS, Wahlestedt C (2010) Adult neurogenesis: A potential tool for early diagnosis in Alzheimer's disease? *J Alzheimers Dis* **20**, 395-408.

[30] Ramos-Cejudo J, Wisniewski T, Marmar C, Zetterberg H, Blennow K, de Leon MJ, Fossati S (2018) Traumatic brain injury and Alzheimer's disease: The cerebrovascular link. *EBioMedicine* **28**, 21-30.

[31] Weber MT, Arena JD, Xiao R, Wolf JA, Johnson VE (2019) CLARITY reveals a more protracted temporal course of axon swelling and disconnection than previously described following traumatic brain injury. *Brain Pathol* **29**, 437-450.

[32] Collins JM, King AE, Woodhouse A, Kirkcaldie M, Vickers J (2019) Age moderates the effects of traumatic brain injury on beta-amyloid plaque load in APP/PS1 mice. *J Neurotrauma* **36**, 1876-1889.

[33] De Strooper B, Karran E (2016) The cellular phase of Alzheimer's disease. *Cell* **164**, 603-615.

[34] Lannfelt L, Pettersson FE, Nilsson LN (2010) Translating research on brain aging into public health: A new type of immunotherapy for Alzheimer's disease. *Nutr Rev* **68**(Suppl 2), S128-134.

[35] Appelqvist H, Waster P, Kagedal K, Ollinger K (2013) The lysosome: From waste bag to potential therapeutic target. *J Mol Cell Biol* **5**, 214-226.

[36] Nixon RA, Yang DS, Lee JH (2008) Neurodegenerative lysosomal disorders: A continuum from development to late age. *Autophagy* **4**, 590-599.

[37] Braak H, Braak E (1991) Demonstration of amyloid deposits and neurofibrillary changes in whole brain sections. *Brain Pathol* **1**, 213-216.

[38] Laforce R Jr, Soucy JP, Sellami L, Dallaire-Theroux C, Brunet F, Bergeron D, Miller BL, Ossenkoppele R (2018) Molecular imaging in dementia: Past, present, and future. *Alzheimers Dement* **14**, 1522-1552.

[39] Ramlackhansingh AF, Brooks DJ, Greenwood RJ, Bose SK, Turkheimer FE, Kinnunen KM, Gentleman S, Heckemann RA, Gunanayagam K, Gelosa G, Sharp DJ (2011) Inflammation after trauma: Microglial activation and traumatic brain injury. *Ann Neurol* **70**, 374-383.

[40] Perry DC, Sturm VE, Peterson MJ, Pieper CF, Bullock T, Boeve BF, Miller BL, Guskiewicz KM, Berger MS, Kramer JH, Welsh-Bohmer KA (2016) Association of traumatic brain injury with subsequent neurological and psychiatric disease: A meta-analysis. *J Neurosurg* **124**, 511-526.

[41] Tarasoff-Conway JM, Carare RO, Osorio RS, Glodzik L, Butler T, Fieremans E, Axel L, Rusinek H, Nicholson C, Zlokovic BV, Frangione B, Blennow K, Menard J, Zetterberg H, Wisniewski T, de Leon MJ (2015) Clearance systems in the brain-implications for Alzheimer disease. *Nat Rev Neurol* **11**, 457-470.

[42] Sollvander S, Nikitidou E, Brolin R, Soderberg L, Sehlin D, Lannfelt L, Erlandsson A (2016) Accumulation of amyloid-beta by astrocytes result in enlarged endosomes and microvesicle-induced apoptosis of neurons. *Mol Neurodegener* **11**, 38.

[43] Kelly KM, Miller ER, Lepsveridze E, Kharlamov EA, McHedlishvili Z (2015) Posttraumatic seizures and epilepsy in adult rats after controlled cortical impact. *Epilepsy Res* **117**, 104-116.

[44] Guo D, Zeng L, Brody DL, Wong M (2013) Rapamycin attenuates the development of posttraumatic epilepsy in a mouse model of traumatic brain injury. *PLoS One* **8**, e64078.

[45] Glushakov AV, Glushakova OY, Dore S, Carney PR, Hayes RL (2016) Animal models of posttraumatic seizures and epilepsy. *Methods Mol Biol* **1462**, 481-519.

[46] Filley CM, Kelly JP (2018) White matter and cognition in traumatic brain injury. *J Alzheimers Dis* **65**, 345-362.

[47] Kokiko-Cochran ON, Godbout JP (2018) The inflammatory continuum of traumatic brain injury and Alzheimer's disease. *Front Immunol* **9**, 672.

[48] Wood RL (2017) Accelerated cognitive aging following severe traumatic brain injury: A review. *Brain Inj* **31**, 1270-1278.

[49] Gold EM, Vasilevko V, Hasselmann J, Tiefenthaler C, Hoa D, Ranawaka K, Cribbs DH, Cummings BJ (2018) Repeated mild closed head injuries induce long-term white matter pathology and neuronal loss that are correlated with behavioral deficits. *ASN Neuro* **10**, 1759091418781921.

[50] Huang YA, Zhou B, Wernig M, Sudhof TC (2017) ApoE2, ApoE3, and ApoE4 differentially stimulate APP transcription and Abeta secretion. *Cell* **168**, 427-441 e421.

[51] Hartman RE, Laurer H, Longhi L, Bales KR, Paul SM, McIntosh TK, Holtzman DM (2002) Apolipoprotein E4 influences amyloid deposition but not cell loss after traumatic brain injury in a mouse model of Alzheimer's disease. *J Neurosci* **22**, 10083-10087.

[52] Powell MA, Black RT, Smith TL, Reeves TM, Phillips LL (2018) Mild fluid percussion injury induces diffuse axonal damage and reactive synaptic plasticity in the mouse olfactory bulb. *Neuroscience* **371**, 106-118.

[53] Ekmark-Lewen S, Flygt J, Kiwanuka O, Meyerson BJ, Lewen A, Hillered L, Marklund N (2013) Traumatic axonal injury in the mouse is accompanied by a dynamic inflammatory response, astroglial reactivity and complex behavioral changes. *J Neuroinflammation* **10**, 44.

[54] Olsen M, Aguilar X, Sehlin D, Fang XT, Antoni G, Erlandsson A, Syvanen S (2018) Astroglial responses to amyloid-beta progression in a mouse model of Alzheimer's disease. *Mol Imaging Biol* **20**, 605-614.

[55] Sirko S, Behrendt G, Johansson PA, Tripathi P, Costa M, Bek S, Heinrich C, Tiedt S, Colak D, Dichgans M, Fischer IR, Plesnila N, Staufenbiel M, Haass C, Snapyan M, Saghatelyan A, Tsai LH, Fischer A, Grobe K, Dimou L, Gotz M (2013) Reactive glia in the injured brain acquire stem cell properties in response to sonic hedgehog. [corrected]. *Cell Stem Cell* **12**, 426-439.

[56] Chun H, Lee CJ (2018) Reactive astrocytes in Alzheimer's disease: A double-edged sword. *Neurosci Res* **126**, 44-52.

[57] Sofroniew MV, Vinters HV (2010) Astrocytes: Biology and pathology. *Acta Neuropathol* **119**, 7-35.

[58] Verkhratsky A, Nedergaard M, Hertz L (2015) Why are astrocytes important? *Neurochem Res* **40**, 389-401.

[59] Nikitidou E, Khoonsari PE, Shevchenko G, Ingelsson M, Kultima K, Erlandsson A (2017) Increased release of apolipoprotein e in extracellular vesicles following amyloid-beta protofibril exposure of neuroglial co-cultures. *J Alzheimers Dis* **60**, 305-321.

[60] Acosta SA, Tajiri N, Sanberg PR, Kaneko Y, Borlongan CV (2017) Increased amyloid precursor protein and tau expression manifests as key secondary cell death in chronic traumatic brain injury. *J Cell Physiol* **232**, 665-677.